STEM CELLS AND DEVELOPMENT
Volume 24, Number 1, 2015

DOI: 10.1089/scd.2014.0135

Systemic Injection of CD34$^+$-Enriched Human Cord Blood Cells Modulates Poststroke Neural and Glial Response in a Sex-Dependent Manner in CD1 Mice

Shilpa D. Kadam,[1,2] HuiGen Chen,[1,3,†] Geoffrey J. Markowitz,[1,3,‡] Saba Raja,[1,3,§] Shanu George,[1,3,**] Elisabeth Shotwell,[1] Brett Loechelt,[4] Michael V. Johnston,[1,2,5,6] Naynesh Kamani,[4,††] Ali Fatemi,[1,2,5] and Anne M. Comi[1,2,5]

Stroke in the developing brain is an important cause of neurological morbidity. We determined the impact of human cord blood-derived CD34$^+$-enriched mononuclear cells (CBSC) intraperitoneally injected 48 h after an ischemic stroke at postnatal day 12 by evaluating poststroke neurogenic niche proliferation, glial response, and recovery in CD1 mice. Percent brain atrophy was quantified from Nissl-stained sections. Density of BrdU, Iba-1, and GFAP staining were quantified in the dentate gyrus and the subventricular zone (SVZ). Immunohistochemistry for human nuclear antibody, human mitochondrial antibody, and human CD34$^+$ cells was done on injured and uninjured brains from CBSC- and vehicle-treated mice. Developmental neurobehavioral milestones were evaluated pre- and post-treatment. No significant differences in stroke severity were noted between CBSC and vehicle-treated injured animals. With a 1×10^5 CBSC dose, there was a significant increase in subgranular zone (SGZ) proliferation in the CBSC-versus vehicle-treated stroke-injured male mice. SVZ glial fibrillary acidic protein (GFAP) expression was increased contralaterally in injured females treated with CBSC but suppressed in injured males. Significant negative correlations between severity of the stroke-injury and spleen weights, and between spleen weights and SGZ proliferation, and a positive correlation between GFAP expression and severity of brain injury were noted in the vehicle-treated injured mice but not in the CBSC-treated mice. GFAP expression and SVZ proliferation were positively correlated. In conclusion, neurogenic niche proliferation and glial brain responses to CBSC after neonatal stroke may involve interactions with the spleen and are sex dependent.

Introduction

Ischemic stroke in neonates and infants can result in long-term cognitive and functional impairments [1]. The clinical presentation is often more subtle than in adults. This leads to a delay in diagnosis and limits the opportunity for acute interventions such as thrombolysis and other neuroprotective strategies. Therefore, strategies aimed at improving recovery and enhancing regeneration after pediatric strokes are needed. Stem cell therapy is currently greatly debated as potential treatment for acute injury to the brain [2]. Human CD34 antigen-positive hematopoietic stem cells (CD34$^+$) comprise the largest fraction of stem cells derived from cord blood (CB). They have been shown to secrete numerous angiogenic factors including VEGF and IGF-1 [3]. The chemokine receptor CXCR4 is expressed on CD34$^+$ pluripotent progenitors, and may play an important role in the homing of hematopoietic stem cells via chemotaxis to acute brain injury sites [4,5]. Clinical safety treatment trials are currently underway with human CB in human infants http://clinicaltrials.gov/ct2/show/NCT00593242 (including a currently recruiting trial of CD34$^+$-enriched autologous CB cells for neonates injured by hypoxia-ischemia (clinical trials.gov identifier number NCT01506258). More preclinical studies are needed to understand the mechanisms of their effects.

Departments of [1]Neurology and Developmental Medicine, Kennedy Krieger Research Institute, Baltimore, Maryland.
Departments of [2]Neurology, [3]Neuroscience, and [5]Pediatrics, Johns Hopkins University School of Medicine, Baltimore, Maryland.
[4]Division of Blood and Marrow Transplant and Immunology, Children's National Medical Center, Washington, District of Columbia.
[6]Physical Medicine and rehabilitation, Johns Hopkins School of Medicine, Baltimore, Maryland.
[†]Current affiliation: Department of Cell and Developmental Biology, Weill Cornell Medical College, New York, New York.
[‡]Current affiliation: Department of Pharmacology and Cancer Biology, Levine Science Research Center, Duke University, Durham, North Carolina.
[§]Current affiliation: St. George's University Medical School, Grenada, West Indies.
[**]Current affiliation: Department of Physiology and Neurobiology, University of Connecticut, Storrs, Connecticut.
[††]Current affiliation: AABB Center for Cellular Therapies, Bethesda, Maryland.

The aim of this study was to investigate the effects of $CD34^+$-enriched hematopoietic stem cells derived from fresh human CB units on early poststroke neurogenic niche proliferation, injury, and glial response in an immature mouse model when delivered systemically 48 h after an ischemic stroke. Developmental neurobehavioral milestones were evaluated pre- and post-treatment. Immunohistological examination of brain sections was done to look for human cells in the fixed mouse tissues after systemic delivery.

Materials and Methods

All research was conducted according to a protocol approved by the Johns Hopkins University School of Medicine Animal Care and Use Committee (IACUC). Newborn litters of CD1 mice were ordered from Charles River Laboratories, Inc. and were allowed to acclimate for 7 days. Anonymized research CB units were obtained and processed at Children's National Medical Center under an IRB-approved protocol.

Surgical procedure for ischemic model

On the morning of P12, equal numbers of male and female animals (Table 1) were subjected to modified Levine procedure (unilateral carotid ligation only) for producing ischemic brain injury as previously described under isoflurane anesthesia [6,7]. Previous studies have demonstrated that early cortical reperfusion occurs in the carotid ligation model [8], thereby mimicking the clinical situation in patients. The animals were allowed to recover in a 37°C chamber for 4 h and acute seizures were scored.

Acute seizure scoring

Acute postligation seizure activity was scored according to a seizure rating scale as previously reported [6,9].

Harvesting $CD34^+$ cells from fresh units of human CB

Fresh umbilical human CB units, designated as research units failing to meet criteria for storage for clinical use, were obtained from a regional public CB collection program. Mononuclear cell layer was harvested after ficoll-hypaque centrifugation, resuspended in Plasma Lyte A, and counted using Sysmex KX-21N. After repeated washes, the cell pellet was resuspended in Running Buffer (Miltenyi Biotec, Inc.) and FcR Blocking Reagent (Miltenyi Biotec, Inc.) followed by incubation with cold CD34 Microbeads (Miltenyi Biotec, Inc.) for 30 min at 4°C–8°C. Resuspended cells were filtered using 30 μm Preseparation Filter (Miltenyi Biotec, Inc.), loaded onto the Miltenyi AutoMACS (Miltenyi Biotec, Inc.) cell separator. The separated product was assayed by flow cytometry (BD FACSCalibur) using CD45 FITC, CD34 PE, and 7-amino-actinomycin D (7AAD) viability dye (Beckmen Coulter) to evaluate total number of leukocytes, $CD34^+$ cells, and viability, respectively. Percent enrichment of the $CD34^+$ CBSCs ranged from 60% to 91%.

Table 1. Numbers of Mice for Each Set of Experiments

	Vehicle	*Cell*
Randomly assigned to each group, *n*	7 females, 9 males	12 females, 9 males
Mortality after treatment, *n*	0 females, 2 males	2 females, 1 male
Surviving to perfusion, *n*	7 females, 7 males	10 females, 8 males
Stroke-injured at P21, *n* (%)	10 (71)	12 (67)
Injured, *n*	5 females, 5 males	6 females, 6 males
Uninjured, *n*	2 females, 2 males	4 females, 2 males

CBSCs were sent on ice and received the same day (P14) by the laboratory performing the injections. CBSC viability was evaluated again immediately prior to injection on P14 (trypan blue). Animals with acute seizures were divided between CBSC-treated and vehicle-treated groups so that animals with matched seizure scores were evenly represented in the two groups. The rest of the animals were randomly distributed between the two groups with the two groups matched for animal sex. Prior pilot studies were done injecting 5×10^4 $CD34^+$ enriched cells and demonstrated no impact upon injury, neurogenesis, or spleen size (data not shown), and therefore the studies reported here were done with a dose of 1×10^5 $CD34^+$-enriched cells. Animals received viability normalized CBSC dosages at concentrations of 1×10^5 CBSCs in a volume of between 70–90 μL. CBSCs or vehicle were injected i.p. manually over a period of 1 min under isoflurane anesthesia. CBSCs and vehicle were stored in an incubation chamber at 36°C before injections and at room air during injection of samples.

Developmental milestones

All pups were scored using developmental milestone guidelines in newborn mice from Hill et al. [10], on P9, P12, P13, P14, P15, P16, P19, and P21 as follows: (1) *Weight gain* with age. (2) *Open-field*: The mouse pup was placed on a sheet of paper in the center of a circle 5'' and 10'' in diameter. The length of time the mouse took to move out of the circles was recorded and graded. If the mouse did not move outside the circles within 30 s, the test was terminated and assigned a fail grade. (3) *Geotaxis*: Each pup was placed on an inclined plane at 45° angle, in a head-down starting position. After placement on the plane, the pup was gently held in the starting position for 5 s before being released and observed for at least 30 s, or until the pup fell or touched a side or bottom wall of the inclined plane. (4) *Forelimb grasp*: The pup was held with its forepaws resting on a small rod suspended over cotton 10 cm deep until it grasped the rod. The pup was then released, and the length of time the pup remained gripping the rod was measured. The test was repeated thrice and highest score noted. See Table 2 for details.

BrdU labeling of postischemia neurogenesis

BrdU (50 mg/kg, i.p.) solution at a concentration of 30 mg/mL was administered 2 h prior to the P21 perfusion fixation. Animals were anesthetized with chloral hydrate (90 mg/kg) and transcardially perfused with 10% formalin and the brains removed. The brains were postfixed in the same fixative for 5 days, cryoprotected in 15% sucrose in PBS for 24 h and 30% sucrose in PBS for 24 h, snap-frozen in dry-ice, and stored at −80°C.

Table 2. Behavioral Tests: Grading Scores

Open-field test		
Time to cross	*Time to cross*	*Score*
5''circle (s)	10''circle(s)	
≥30 (Fail)	≥30 (Fail)	1
<30	≥30 (Fail)	2
15 to <30	<30	3
10 to <15	<30	4
5 to <10	<30	5
>2 to <5	<30	6
0 to 2	<30	7

Geotaxis test	
Time taken to turn left or right from starting position (s)	*Score*
>30 (Fail)	0
20 to 30	1
10 to <20	2
5 to <10	3
0 to <5	4
Scores 5–9 refer to the pup moving outside the inclined plane and the direction to which it moves with eyes open or closed.	
Top/Side-eyes open	5
Top/Side-eyes closed	6
Bottom-eyes open	7
Bottom-eyes closed	8
Exploring without specific Direction-eyes open	9
Once the pup's eyes open, only a score from 5 to 9 may be used. If the pup fails to turn within 30 s, a score of 0 is assigned.	

Forelimb grasp test	
Time pup holds onto string with forelimbs (s)	*Score*
No grasp (Fail)	0
>0 to 2	1
>2 to <5	2
5 to <15	3
15 to <30	4
≥30	5
Time taken to go to port ≥20	6
Time taken to go to port 15 to <20	7
Time taken to go to port 10 to <15	8
Time taken to go to port 5 to <10	9
Time taken to go to port 0 to <5	10

If the pup climbs to either end of the string, it has reached ''port'' and is scored by time taken to reach ''port.'' A higher score then indicates lower time taken to travel to the end of the string.

Histology

Forty micrometers thick coronal brain sections were cut in six series on a cryostat and mounted on super frost plus glass slides. A range of injury occurs in this model, from micro (ie, tiny patches of cell death and gliosis in the hippocampus, without atrophy) to macro lesions (ie, massive infarcts forming porencephalic cysts). Cresyl-violet-stained sections were microscopically examined to determine the severity of injury in brains without an obvious stroke lesion. One brain had microscopic injury; this was a vehicle-treated animal that was excluded as an outlier. Ligation-uninjured were classified as mice having no discernible stroke-injury on either macroscopic or microscopic examination.

Computerized measurement of atrophy and subgranular zone length

Brain atrophy measurements were done as previously described [9] using MCID 7.0 Elite (InterFocus Imaging Ltd.) to measure hemispheric areas of Nissl-stained coronal serial sections spanning rostral striatum to caudal hippocampus ($n = 10$–12 sections per animal). Total subgranular zone (SGZ) lengths were measured by tracing the SGZ contours using MCID in every DG in which SGZ BrdU-positive cells were quantified.

Immunohistochemistry

After blocking for nonspecific reactions the slide-mounted tissue sections were sequentially incubated overnight in 4°C with primary antisera that included HuNu (MAB1281; Human Anti-Nuclei, clone 235; 1:100; Millipore), HuMit (MAB1273; Human Anti-Mitochondria, surface of intact mitochondria, clone 113; 1:100; Millipore), CD68 (ab53444; Rat anti-mouse CD68; 1:100; abcam), rabbit anti-CD34 (Epitomics, 1:500), GFAP (glial fibrillary acidic protein; Rabbit anti-GFAP; 1:20; Immunostar, Catalog No. 22522), Iba-1 (ionized calcium binding adaptor molecule 1; Goat anti-iba-1; 1:500; Abcam, Catalog No. ab5076), or mouse anti-BrdU monoclonal antibody (1:200; Roche). For BrdU immunohistochemistry, the DNA was denatured with 2N HCL for 30 min at 37°C. Secondary antibodies sequentially used were Alexa 594 and Alexa 488 conjugated and incubated for 1 h at room temperature. Nuclei were stained with Hoechst (Invitrogen). Slides were coverslipped with prolong antifade medium.

Detection of human cells in the mouse brain

Researcher analyzing slides for human cells were blinded to treatment group and visualized using the AxioVision Apotome System (Carl Zeiss MicroImaging). The ipsilateral (right hemisphere) side of each section was examined by manually scanning through tissue in a grid-like pattern at 20× and at the 488 wavelength. Cell-like structures were imaged at 63× and added to analysis if they met criteria: (1) being human mitochondrial and DAPI co-labeled and spherical in shape OR (2) being spherical in shape, triple stained (HuNu, CD34$^+$, and Dapi$^+$), and between 1 and 6 μm in diameter. Images were then analyzed by using the diameter measure (μm) for each cell-like structure using AxioVision Apotome System Software. Samples were decoded and grouped into one of four categories: vehicle-treated injured, vehicle-treated uninjured, cell-treated injured, or cell-treated uninjured. Averages and standard deviations were calculated.

Microscopy

All quantification was done by investigators blinded to animal identification and treatment assignments. A method described previously [9] was used to estimate total counts of

BrdU-positive cells in six consecutive coronal serial sections from the dorsal hippocampi. Total counts in each section were normalized to the GCL length (ie, cells/mm length of corresponding SGZs) and mean densities reported. In addition, because rostral to caudal differences in neurogenesis after ischemia have been suggested in the literature [11] an analysis of SGZ BrdU counts was performed with respect to the rostro-caudal axis of the mouse brain. Iba-1-positive cells in the hilus and SGZ were quantified using fluorescence microscope 20× objective as previously described [9] in six equally spaced sections adjacent to the sections in which BrdU-positive cells were quantified.

For quantification of GFAP expression in the DG, five 2 μm z-stack images of GFAP and DAPI-labeled sections were acquired using Axio Imager M2 microscope at 10× magnification using a mosaic montage of three by three images and collapsed in a single image. The DG was subdivided into the GCL and the hilar regions. Images inverted in Adobe Photoshop CS4 software (Adobe Systems Incorporated) granularly segmented to separate GFAP-positive area from GFAP-negative area and then the immunopositive area in each region of interest was measured (Fig. 1A–C) using MCID 7.0 Elite software (InterFocus Imaging Ltd.).

Stacks of 1 μm thick images of BrdU and GFAP in the subventricular zone (SVZ) region were taken on an Olympus FV 1000 laser scanning confocal system at bregma coordinates level 0.74 to 1.18 mm [12]. Images were analyzed using Image J (U.S. National Institutes of Health; http://rsb.info.nih.gov/ij/, 1997–2006) software to arbitrarily quantify BrdU, and GFAP expression, in the region of the SVZ of ligated and control brains as previously reported [13]. The SVZ region was further subdivided into the SVZ proper, the white matter above the SVZ, and the striatum below the SVZ, and BrdU and GFAP labeling was quantified in these regions using MCID; standardized distances from the SVZ (Fig. 1D–F) to outline regions of interest and measure proportional target areas.

To quantify Iba-1labeling in the SVZ, five 4 μm z-stack images of Iba-1 and DAPI labeled sections were acquired using Axio Imager M2 microscope at 10× magnification. Analysis of the antero-rostral trigone of the SVZ at bregma coordinates 0.74 to 1.18 mm [12] was done. The z-stacks were kept uncollapsed for ease of counting individual cells throughout the stack using AxioVision 4.8 software (Carl Zeiss Imaging Solutions GmbH). DAPI-stained images were used for identification of the structure of interest (Fig. 1G–I).

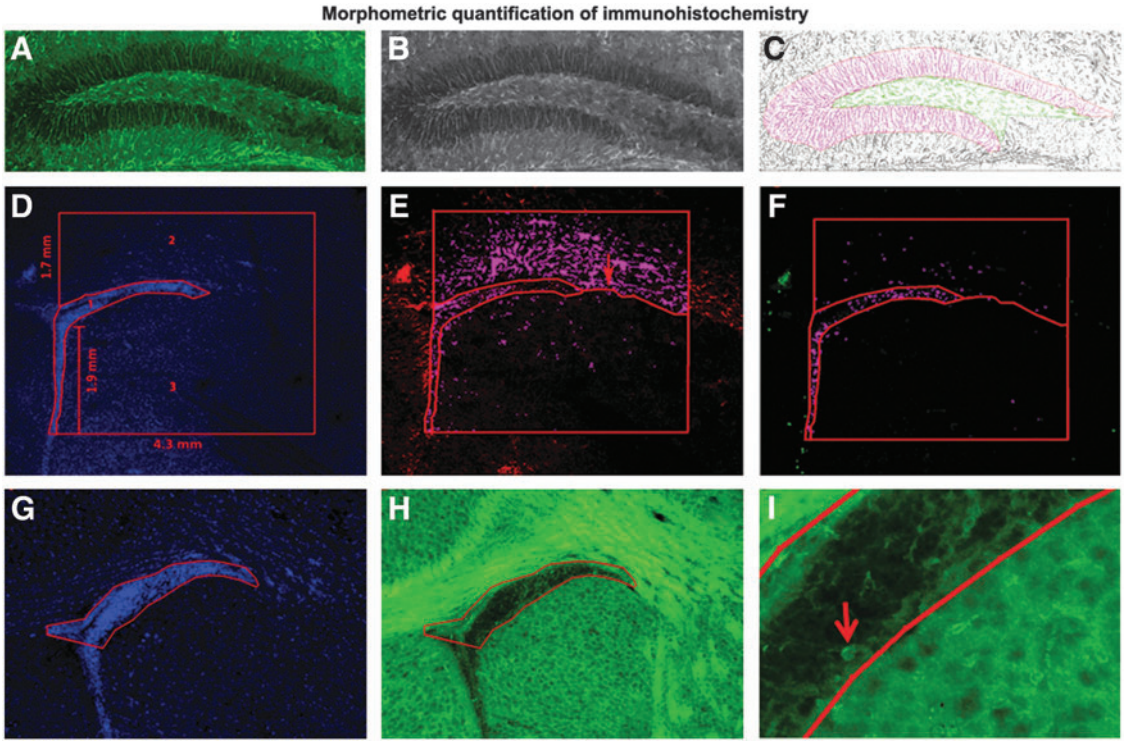

FIG. 1. Morphometric quantification of immunohistochemistry. **(A–C)** Quantification of glial fibrillary acidic protein (GFAP) expression in the granule cell layer and hilus of the dentate gyrus. Color images of GFAP immunolabeling **(A)** were converted to *black* and *white* **(B)** and then inverted in Adobe Photoshop. The dentate gyrus (DG) was subdivided into the granule cell layer (GCL) and the hilar regions, and immunopositive area was quantified **(C)** using MCID software. **(D–F)** Quantification of BrdU and GFAP expression in the subventricular zone (SVZ) proper, white matter dorsal to SVZ, and the striatum below the SVZ. The regions of interest were outlined using MCID software on DAPI-stained sections images taken at 10× and using the parameters indicated in **(D)**. A line separating the striatum from white matter was drawn in linked images from GFAP-stained sections **(E)** and GFAP immunopositive proportional target area quantified in the three regions of interest. Then BrdU proportional target area was quantified in linked images from BrdU-stained sections **(F)**. **(G–I)** Quantification of density of Iba-1-labeled cells in the SVZ. The SVZ was outlined using Axiovision software on DAPI-stained sections images taken at 10× and **(G)** linked to Iba-1-stained images **(H, I)** in which the number of Iba-1-labeled cells **(I,** *arrow***)** in the SVZ were counted.

Methods of analysis

Statistical analyses were run in SPSS for Windows (SPSS, Inc.). Repeated measures ANOVAs were carried out to analyze scores for developmental milestones. Two-way ANOVA (Sex by Treatment) analysis and *t*-tests were done for the percent atrophy and immunohistochemistry data for the ipsi- and contralateral sides in the ligation-injured group of CBSC- and vehicle-treated mice. The rostro-caudal distribution of BrdU positive cells was analyzed using a marginal generalized linear model with Poisson distribution and generalized estimating equations to account for clustering of sections within treated versus untreated mice [14]. Correlations were reported whenever statistical significance was noted. Mean ± SEMs were reported and a probability below 0.05 was considered significant.

Results

Forty-seven pups (including 10 naïve controls) of both sexes were utilized from 7 L of CD1 mice (see Table 2 for details). About 16/37 (43.2%) of the animals seized acutely and seizure scores were used to distribute similar brain injury between the two treatment groups. The overall post-treatment mortality in the study was 13.5% (n/n = 5/37); 12.5% vehicle-treated versus 14.3% CBSC-treated (N.S). 68.8% (n/n = 22/32) of the P12-ligated CD1 mice that survived to the P21 perfusion time point were injured and 34.4% (n/n = 11/32) of the surviving animals had acute behavioral seizures.

Weight and developmental milestones as compared to naïve controls

The data demonstrated a consistent and significant lag in weight gain in stroke-injured mice in both vehicle- and CBSC-treated pups (repeated measures ANOVA $P < 0.0005$) compared to shams. The lag in weight gain in stroke-injured mice did not improve with CBSC-treatment (Fig. 2A). Ligation-injury resulted in significantly lowered performance on the open-field test of vehicle-treated and cell-treated injured animals compared with naïve controls (repeated measures ANOVA $P < 0.0005$). However at P21, irrespective of treatment, ligation-injured mice had recovered to scores similar to naïve controls (Fig. 2B) and results on this task were not different between injured and uninjured ligated mice (data not shown). The geotaxis and forelimb grasp tests did not reveal significant impairments in the immature stroke-injured mice irrespective of treatment (Fig. 2C, D respectively).

Severity of stroke injury and spleen weights

No significant differences in stroke severity were detected between CBSC-treated and vehicle-treated groups at P21 (see Fig. 3A, B). In addition, no sex differences were detected (see Fig. 3C, D). Similar to our previous reports, the severity of stroke injury strongly correlated with the severity of acute seizures, including in this study the mice treated with CBSCs ($r^2 = 0.81$ and $P < 0.0005$ for both hippocampal and hemispheric atrophy). The severity of hippocampal atrophy correlated with severity of hemispheric atrophy ($r^2 = 0.84$,

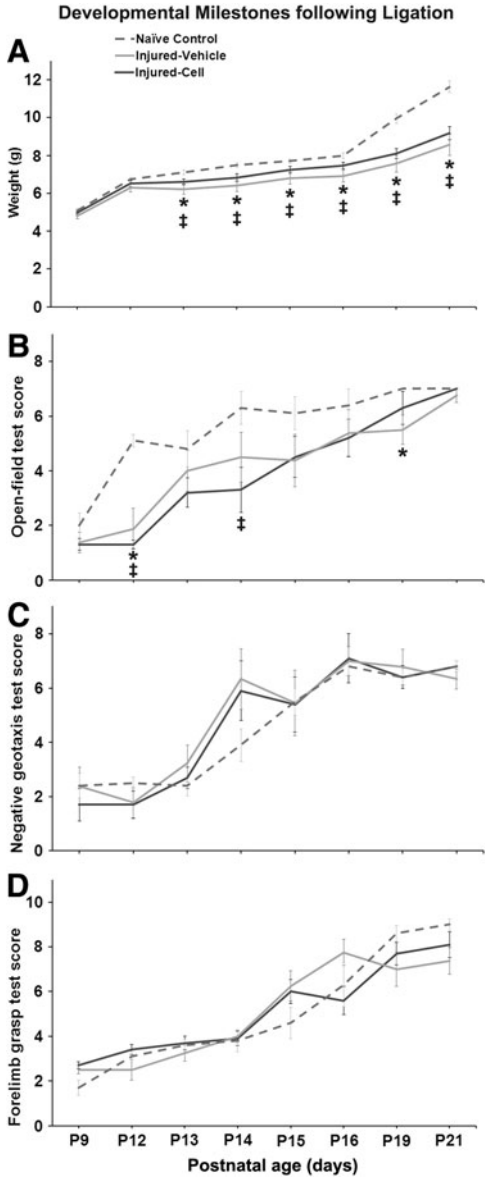

FIG. 2. Developmental milestones following P12 ligation in CD1 mice. **(A)** Poststroke weight gain in ligation-injured CBSC- and vehicle-treated mice compared to naïve controls. Stroke-injured mice showed an age-dependent lag in weight-gain following stroke that remained significant at P21 ($P < 0.05$) among both injured CBSC- (*) and vehicle-treated mice (‡). This lag did not show improvement in the CBSC-treated group of injured-mice when compared to the vehicle-treated group of injured mice. **(B)** Open-field: stroke-injured mice showed a delayed progress in open-field activity compared with naïve controls ($P < 0.05$); however, by P21 they were not significantly different from controls; ligation-uninjured animals ($n = 8$; three vehicle-treated and five CBSC-treated) were not, however, significantly different from ligation-injured animals (data not shown). CBSC-treated injured mice did not show significant improvements in open-field activity compared to the vehicle-treated group in the 7 day follow-up after treatment (ie, P14- P21). **(C)** Geotaxis: milestones for negative geotaxis scores were not significantly different in ligation-injured mice compared to naïve controls irrespective of treatment. **(D)** Forelimb grasp milestones were not significantly affected in the ligation-injured mice irrespective of treatment.

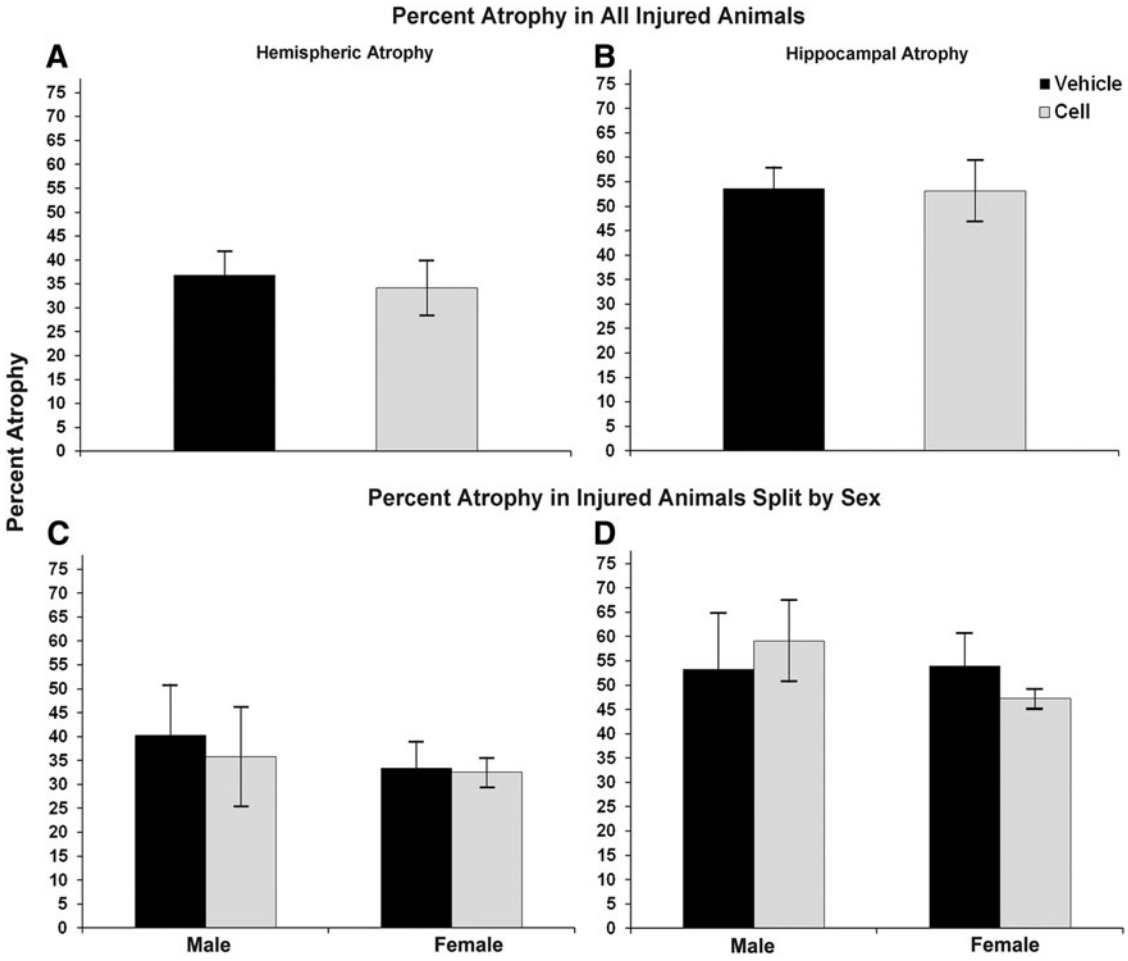

FIG. 3. Severity of infarct injury following P12 ligations quantified at P21 (7 days following treatment with CBSC or vehicle at P14; **A and B**). No significant differences were noted in either hemispheric (*left*) or hippocampal atrophy (*right*) between CBSC-treated and vehicle-treated groups either when all animals were analyzed together **(A, B)** or when analyzed by animal sex **(C, D)**.

$P < 0.0005$ CBSC-treated and $r^2 = 0.91$, $P < 0.0005$ vehicle-treated).

Severity of stroke injury at P21 negatively correlated with spleen weights in the injured vehicle-treated mice ($r^2 = -0.76$, $P < 0.05$ hemispheric atrophy and $r^2 = -0.83$, $P < 0.02$ hippocampal atrophy). CBSC-treated injured mice did not demonstrate significant negative correlations between injury and spleen weights ($r^2 = -0.30$, $P = 0.40$ and $r^2 = -0.61$, $P = 0.06$ hemispheric and hippocampal respectively). Ipsilateral SGZ cell proliferation strongly correlated with spleen weights in the vehicle-treated injured animals ($r^2 = -0.93$, $P < 0.005$) as did contralateral SVZ proliferation ($r^2 = 0.76$, $P < 0.05$); spleen weight did not similarly correlate with neurogenic niche cell proliferation in CBSC-treated animals ($r^2 = 0.25$, $P = 0.52$ and $r^2 = -0.02$, $P = 0.96$). Spleen weights also negatively correlated with GFAP expression in the ipsilateral SVZ and in the ipsilateral striatum below the SVZ in the vehicle-treated ($r^2 = -0.79$, $P < 0.05$ and $r^2 = -0.93$, $P < 0.005$ respectively) but not in CBSC-treated injured animals ($r^2 = -0.43$, $P = 0.24$ and $r^2 = -0.22$, $P = 0.58$). Spleen weights did, however, negatively correlate with the density of Iba-1-labeled cells in the ipsilateral SVZ in CBSC-treated animal only ($r^2 = -0.81$, $P < 0.02$ CBSC-treated versus vehicle-treated $r^2 = -0.25$, $P = 0.59$).

Poststroke SGZ cell proliferation and response to treatment was sex dependent after CBSC treatment

The ANOVA analysis for effects of treatment and sex upon BrdU-labeled cell density in the SGZ showed trends for main effects of sex and treatment ($P = 0.06$ and 0.05 respectively, Fig. 4). The sex-specific difference in response to treatment was clearly evident, however, with the rostrocaudal analysis of SGZ BrdU cell densities. This method of analysis accounts for the anatomical relationship between sections and impact of this upon counts (Fig. 4C). The poisson regression analysis was significant in males bilaterally (ratio of density 1.35 contralaterally (range 1.05, 1.74; $P < 0.02$) and 1.32 ipsilaterally (range 1.10–1.60; $P < 0.005$) but not in females (ratio of BrdU density 1.08 contralaterally (range 0.92–1.26; $P = 0.345$) and ipsilaterally 0.95 (range 0.57–1.58; $P = 0.84$).

Analysis of BrdU labeling in the region of the SVZ contralaterally revealed trends for a main effect of sex ($P = 0.075$; Fig. 5) and for a contralateral increase in SVZ

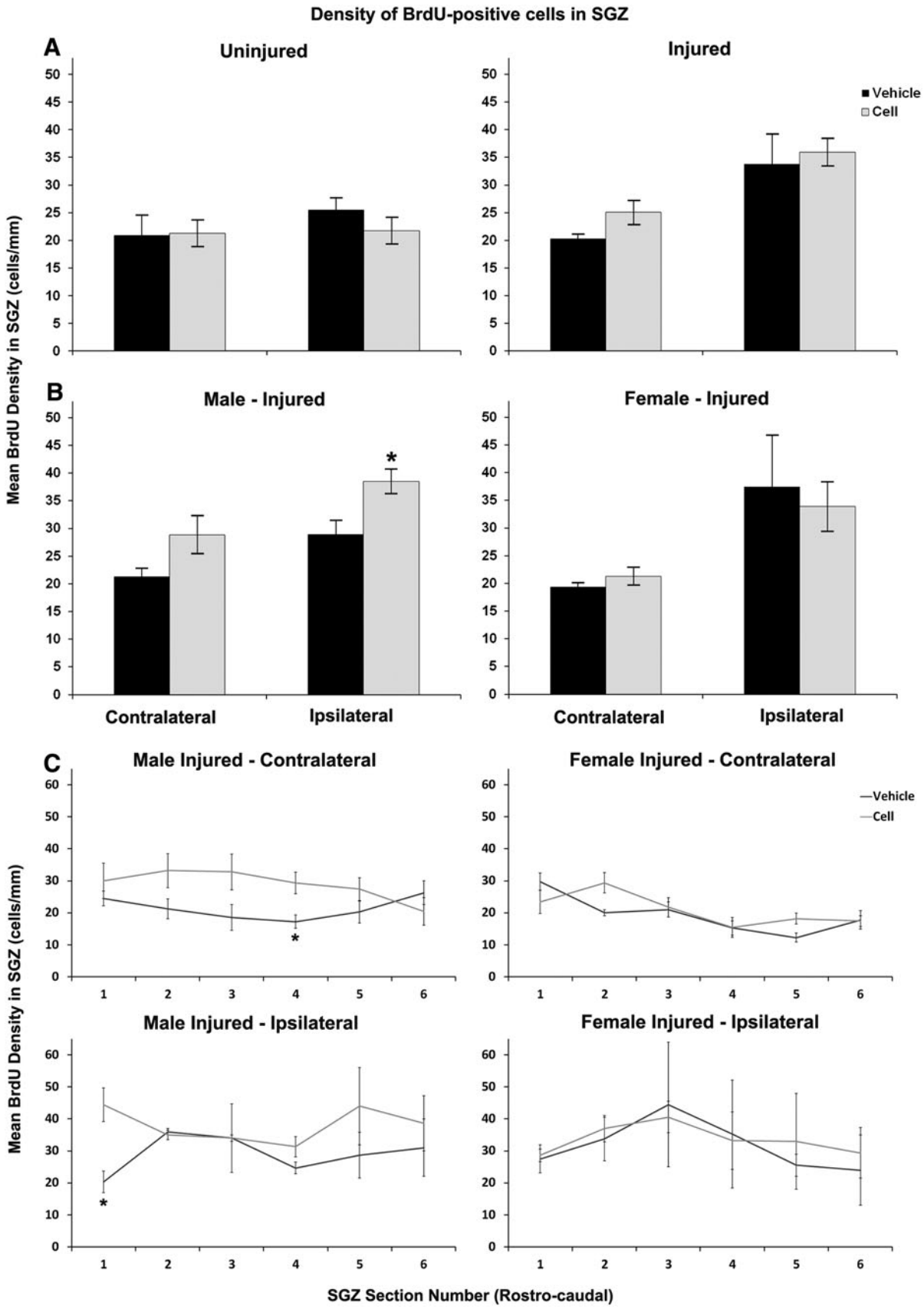

FIG. 4. Density of BrdU-positive cells in the subgranular zone (SGZ) after treatment with vehicle versus CBSC **(A–C).** A nonsignificant ($P = 0.065$) increase was noted in density on the contralateral side of injured animals (**A**-*right*). However, when broken down by animal sex **(B)** this increase was significant and seen only in males ipsilaterally, $P < 0.05$ (**B**-*left*). (**C**) Rostro-caudal analyses by hippocampal section along the AP axis revealed a significant sex difference by Poisson regression (see text, page 6, column 2) in CBSC-treated versus vehicle-treated injured littermates. The upregulation of SGZ proliferation was driven by CBSC-treated males within the data set. ($^*P < 0.05$).

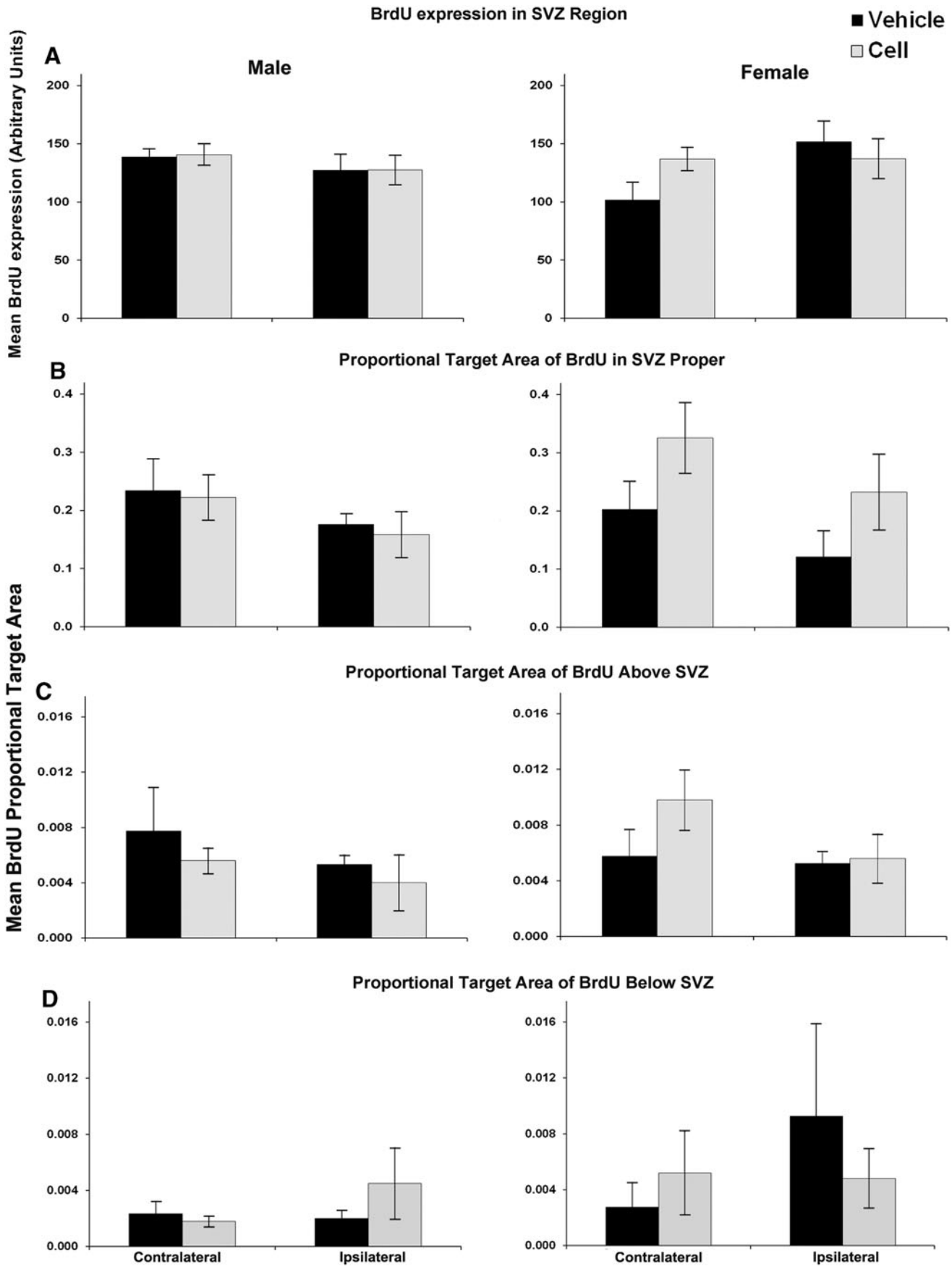

FIG. 5. BrdU expression in the SVZ and surrounding regions of vehicle-treated versus CBSC-treated males (*left*) and female (*right*) injured mice **(A–D).** A nonsignificant increase ($P = 0.085$) was noted in BrdU expression in the contralateral SVZ region in injured females treated with CBSC **(A)**. This trend was mirrored by similar average increases in the contralateral SVZ proper **(B)** and white matter above the SVZ **(C)** of injured females treated with CBSC that did not reach significance.

BrdU labeling in injured females that received CBSC (Fig. 5). Similar increases in the SVZ proper and in the white matter above the SVZ were not significant. In CBSC-treated injured animals, SVZ density of BrdU-labeled cells was positively correlated with GFAP expression in the SVZ bilaterally ($r^2 = 0.75$, $P < 0.02$ contralateral; $r^2 = 0.73$, $P < 0.05$ ipsilateral), in the white matter superior to the SVZ bilaterally ($r^2 = 0.69$, $P < 0.05$ contralateral; $r^2 = 0.68$, $P < 0.05$ ipsilateral) and in the striatum inferior to the SVZ ipsilaterally ($r^2 = 0.80$, $P < 0.02$). These positive correlations were not present in the injured vehicle-treated animals: SVZ GFAP ($r^2 = 0.04$, $P = 0.99$ and $r^2 = -0.61$, $P = 0.15$), white matter GFAP ($r^2 = -0.04$, $P = 0.99$ and $r^2 = -0.39$, $P = 0.38$), and striatum GFAP ($r^2 = -0.28$, $P = 0.54$ and $r^2 = -0.64$, $P = 0.12$).

GFAP expression in the DG and SVZ in response to treatment

GFAP expression in the hilus and granule cell layer of the DG was ipsilaterally increased in stroke-injured animals as compared with uninjured animals (Fig. 6A). However, CBSC treatment did not significantly impact GFAP expression in injured animals compared to vehicle treated. In injured vehicle-treated animals, GFAP expression in the ipsilateral SGZ positively correlated with hemispheric atrophy (GCL and hilus $r^2 = 0.79$, $P < 0.05$). In injured CBSC-treated animals, GFAP expression in the ipsilateral SGZ did not significantly correlate with hemispheric atrophy (GCL $r^2 = 0.52$, $P = 0.18$; hilus $r^2 = 0.48$, $P = 0.23$).

GFAP expression was upregulated in the ipsilateral SVZ of stroke-injured mice compared with the uninjured mice (Fig. 6B) in both CBSC-treated and vehicle-treated animals. Contralaterally, however, it was significantly lower in the vehicle-treated group compared with uninjured animals (Fig. 6B). Severity of brain injury correlated with GFAP expression in the ipsilateral striatum inferior to the SVZ in both vehicle- and CBSC-treated injured animals $r^2 = 0.93$, $P < 0.005$ hippocampal atrophy in vehicle-treated; $r^2 = 0.83$, $P < 0.01$ hemispheric atrophy, and $r^2 = 0.68$, $P < 0.05$ hippocampal atrophy in CBSC-treated). CBSC-treatment overall did not significantly alter GFAP expression, both ipsilaterally or contralaterally, in either injured or uninjured mice when compared with their vehicle-treated counter parts. However, in the CBSC-treated injured animals, the SVZ GFAP expression on the ipsilateral side correlated with that on the contralateral side ($r^2 = 0.75$, $P < 0.05$) suggesting bilateral SVZ glial responses to the injury after the CBSC treatment that were not present in the vehicle-treated animals ($r^2 = -0.32$, $P = 0.48$). A two-way ANOVA for effects of sex and treatment upon GFAP in the SVZ region did not reveal any effects of sex or treatment; however, sex by treatment interaction was significant in the ipsilateral ($P < 0.01$) and contralateral SVZ ($P < 0.05$), and the area above the contralateral SVZ ($P < 0.05$). Injured CBSC-treated females showed significantly higher GFAP expression in the contralateral SVZ region than vehicle-treated females (Fig. 7A). Trends for increased GFAP expression were noted in the SVZ proper and in the white matter above the SVZ, but not in the striatum below the SVZ (Fig. 7B–D). In contrast, similar comparisons in male mice revealed a trend for lower GFAP expression in the SVZ of CBSC-treated males as compared with vehicle-treated males (Fig. 7A). In CBSC-treated animals, injured females had significantly higher GFAP expression in the ipsilateral SVZ compared with males (2751.2 ± 355.3 arbitrary units versus 1595.8 ± 121.5 arbitrary units, $P < 0.05$). In vehicle-treated injured animals females had significantly lower GFAP expression in the white matter dorsal to the contralateral SVZ compared with males (0.125 ± 0.033 arbitrary units versus 0.299 ± 0.057 arbitrary units, $P < 0.05$).

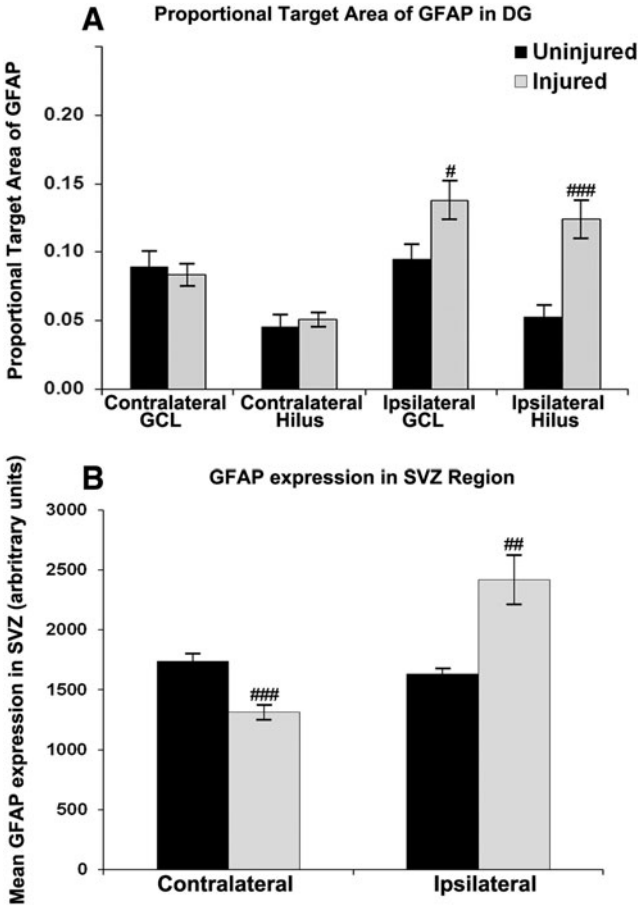

FIG. 6. GFAP expression quantified in the granule cell layer and in the hilus of the dentate gyrus **(A)** and in the subventricular zone (b) of all injured and uninjured mice. GFAP expression was significantly increased ipsilaterally **(A, B)** in both neurogenic niches (GCL $^{\#}P < 0.05$; Hilus $^{\#\#\#}P < 0.0005$; SVZ $^{\#\#}P < 0.002$) and was decreased contralaterally in the SVZ **(B)** 9 days after injury ($^{\#\#\#}P < 0.001$).

Poststroke microglial density in the SGZ/hilus and SVZ

Density of Iba-1-positive cells in the hilus of the ipsilateral DG in all injured hippocampi was increased 9 days after ligation (Fig. 8A) compared with uninjured brains. In addition, the density of Iba-1-labeled hilar cells at P21 positively correlated with hippocampal atrophy in both vehicle- and CBSC-treated animals ($r^2 = 0.86$, $P < 0.02$ and $r^2 = 0.77$, $P < 0.02$ respectively). Both males and females demonstrated an increase in SGZ microglial density compared with uninjured controls. Within the stroke-injured group,

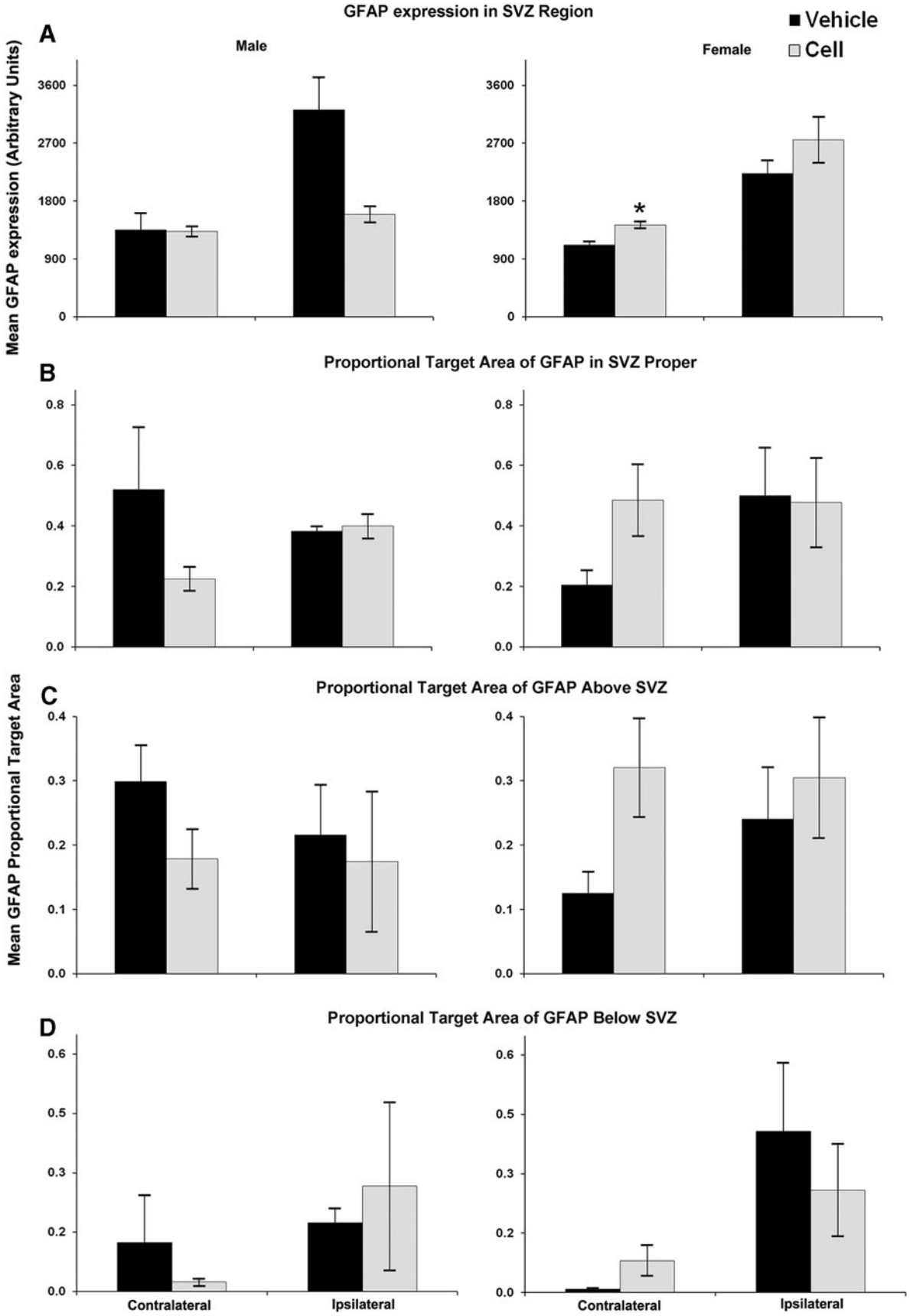

FIG. 7. Quantification of GFAP expression in the SVZ and surrounding regions of vehicle-versus CBSC-treated males (*left*) and female (*right*) injured mice **(A–D).** There was a trend for a decrease in GFAP expression in the SVZ region ipsilaterally in CBSC-treated males ($P = 0.07$; **A**-*left*), while in females GFAP expression in the SVZ region was significantly increased ($P < 0.005$; **A**-*right*). There were also trends for increased GFAP expression in the SVZ itself ($P = 0.08$; **B**-*right*) and in the white matter above the SVZ ($P = 0.06$; **C**-*right*) in injured females treated with CBSC. (*$P < 0.05$).

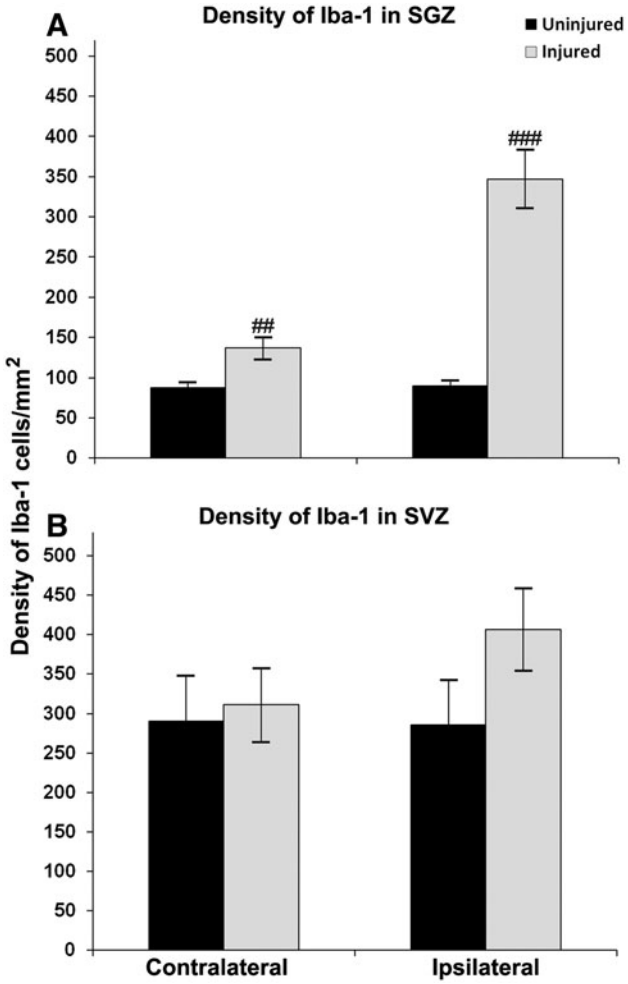

FIG. 8. Density of Iba-1 expression in the SGZ and SVZ of injured versus uninjured mice. Expression of Iba-1 was significantly increased in the SGZ hilus of injured mice after carotid ligation at P12 ($^{###}P<0.000005$ ipsilaterally and $^{##}P<0.005$ contralaterally; **(A)**. Average expression of Iba-1 in the ipsilateral SVZ was increased but not significantly **(B)**.

treatment did not significantly alter Iba-1 density in the hilus of CBSC-treated mice as compared to the vehicle-treated group. Sex did not make any difference in the effect of treatment (data not shown).

Microglial density was higher in the ipsilateral SVZ of all injured mice compared to all uninjured mice but not significantly (Fig. 8B). Within the injured group of mice, CBSC treatment showed no significant effects on microglial density in the ipsilateral or contralateral SVZ trigone when compared to vehicle-treated mice. Sex did not make any difference in the effect of treatment. Density of Iba-1-labeled cells in the ipsilateral SVZ strongly correlated with that in the contralateral SVZ in vehicle-treated injured animals ($r^2=0.86$, $P<0.02$) suggesting bilateral effects of the SVZ microglial response to the injury.

Detection of human cells in stroke-injured brains

HuMit stained sections from both vehicle- and CBSC-treated stroke-injured brains and spleens showed rare counts of HuMit-positive cells (see Fig. 9). MAB 1281 (HuNu) showed many nonspecifically stained cells in the injured brains and spleens of both treated and untreated stroke-injured mice. Staining was only seen at the edge of the infarct core. Anti-mouse CD68 labeling was only seen around infarct edges, and some CD68-positive cells co-labeled with HuMit, both in treated and untreated mice (data not shown). This indicated that a portion of the nonspecific labeling of cells was associated with the endogenous infiltration of macrophages in the infarcted areas. As an additional control, we stained a few brain sections from mice implanted with human glioblastoma cells that showed specific labeling for these human markers; the negative controls remained negative in those brain samples (data not shown).

Of the 29 total brains stained for HuNu, CD34$^+$, and DAPI, cell-like structures were found in seven of the seven vehicle-treated injured (mean diameter 2.76 μm, SD 0.64), two of the four vehicle-treated uninjured (mean diameter 3.81 μm, SD 0.28), 12 of the 12 cell-treated injured (mean diameter 3.02 μm, SD 0.74), and two of the six cell-treated

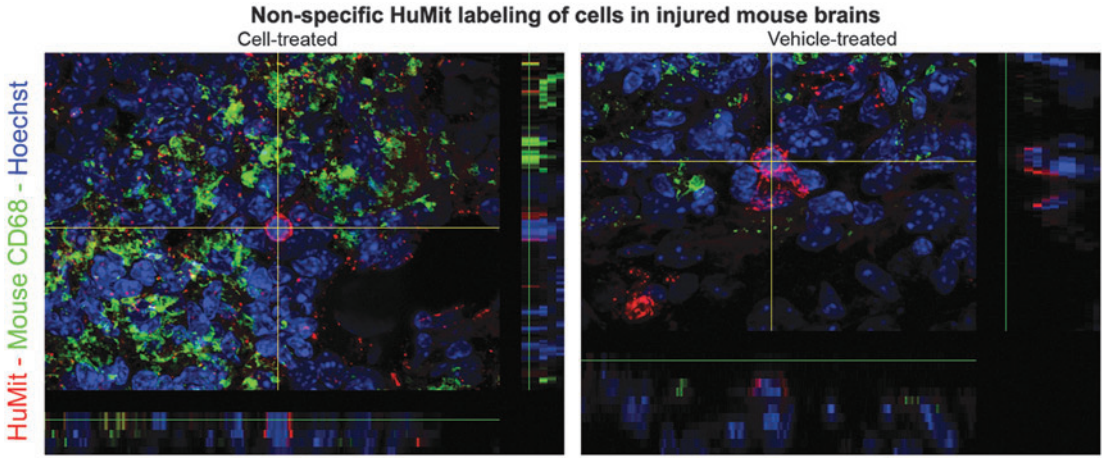

FIG. 9. Confocal images (60×) of fixed coronal brain sections from ipsilateral stroke-injured hemispheres (ie, infarct borders) of ligated mice treated with 1×10^5 CBSC-dosage of CD34$^+$ enriched fraction of human CB cells or vehicle (Plasma Lyte A) stained with mouse-specific anti-CD68 and human mitochondrial (HuMit, MAB 1273) markers. Nonspecific labeling with HuMit antibody was noted in the injured hemispheres of both CBSC and vehicle-treated animals.

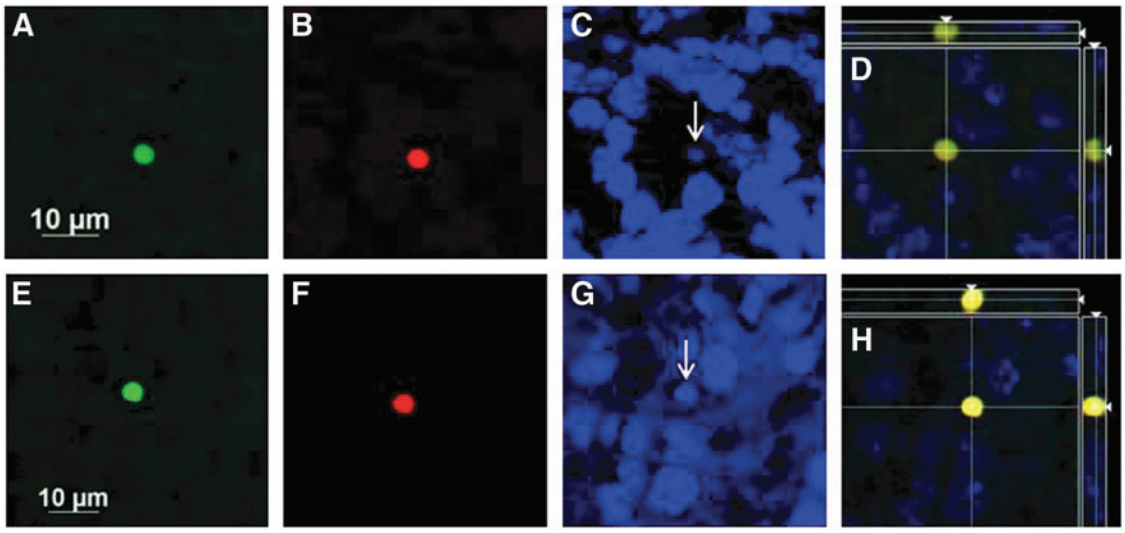

FIG. 10. Apotome images (60×) of fixed coronal brain sections from ipsilateral stroke-injured hemispheres of ligated mice treated with 1×10^5 CBSC-dosage of $CD34^+$-enriched fraction of human CB cells or vehicle (Plasma Lyte A) stained with human nuclear antibody (**A** and **E**, *green*), human $CD34^+$ (**B** and **F**, *red*), and Dapi (*arrow* **C** and **G**, *blue*); merged images (**D** and **H**) demonstrate that double-labeling is imaging the same cell. Nonspecific labeling with antibodies was noted in the injured hemispheres of both CBSC **(A–D)** and vehicle-treated **(E–H)** animals.

uninjured animals (mean diameter 4.06 μm, SD 0.92). Images of the triple-labeled cells were repeatedly reviewed by researchers blinded to the treatment groups. No morphological characteristics could be identified that separated cell treated from vehicle-treated animals (see Fig. 10), or injured from uninjured animals. Many more of these triple-labeled cells were seen in injured animals (11.6 ± 10.4 (SD) triple-labeled cells in cell-treated injured animals, 9.4 ± 12.3 triple-labeled cells in vehicle-treated injured animals versus 1.0 ± 0.0 triple-labeled cells in cell-treated uninjured animals, and 1.5 ± 0.7 triple-labeled cells in vehicle-treated uninjured animals; $P=0.101$) than in uninjured animals.

Discussion

This study demonstrated that i.p. injection of 1×10^5 CBSC 48 h after ligation in an immature mouse model of stroke caused a sex-dependent increase in SGZ cell proliferation in males and suggested an increase in contralateral SVZ cell proliferation in females. Increased cell proliferation in these neurogenic niches was associated with increases in GFAP expression in the SVZ of female mice. Injured animals that received CBSC displayed altered correlations between the spleen weights and severity of injury, and between spleen weights and cell proliferation, and between cell proliferation and GFAP expression, and between GFAP expression and severity of brain injury, compared with vehicle-treated animals.

Prior neonatal studies utilized hypoxia-ischemia models and were performed in rats; this work extends the preclinical field by studying CBSC effects in a mouse model of stroke in the immature brain. The carotid artery is ligated, however, prior studies in both rats and mice measuring cerebral blood flow after the ligation have demonstrated reperfusion within hours of the onset of ischemia thereby mimicking the clinical situation in patients. Furthermore, the P12 CD1 mouse model displays acute behavioral seizures that is an advantage for two reasons: (1) because neonates and infants present with seizures when they have a stroke and (2) because the severity of seizures correlates with the severity of injury in this model, the acute seizures are therefore helpful in ensuring that the distribution of injury within the CBSC and vehicle treatment groups are similar at the time of treatment.

Previously published translational studies in stroke models have demonstrated beneficial effects of the whole mononuclear CB fraction using doses ranging from 1×10^6 to 1×10^7 cells or $CD34^+$-enriched fractions at doses of 1×10^5 [15–17]. The $CD34^+$ stem cell fraction typically comprises ~1% of the CB mononuclear cell fraction [18]; therefore the number of $CD34^+$ cells in the enriched dose (60%–90% $CD34^+$ cells) we administered is within the dose range of $CD34^+$ cells, which has been tested previously. We administered the $CD34^+$-enriched cell fraction to determine more precisely the impact of this CB-derived stem cell fraction, which is currently being studied in a human clinical trial of term neonates exposed to hypoxic-ischemic brain injury. If successful, this approach is likely to be studied in infants after neonatal stroke as well. CBSC are also not ethically an issue as are embryonic sources of stem cells. Furthermore, there is in vitro evidence that these cells may transdifferentiate into neural cells, although it remains unclear whether this occurs in vivo [19].

We chose to administer the CBSC 48 h after ischemic injury to target the processes of inflammation and blood–brain barrier (BBB) opening, which might allow improved accessed to the brain and modifiable processes [20]. Homing of systemically introduced CBSC to injured cortices by chemotaxis may depend on opening of the BBB following stroke-injury in the 24–72 h postischemia and the associated increase in expression of chemokines during the reperfusion phase after ischemia, which may facilitate the migration of systemically grafted cells toward the ischemic core. Other recent studies have

indicated that there is a time window during the first few days after a stroke during which cellular therapy is the most effective [21]. It has been proposed that therapy with hematopoietic stem cells may benefit stroke-injured brains by boosting the release of neurotrophic factors and enhancing cell proliferation in the neurogenic niches of the brain SVZ and SGZ [22,23]. The demonstration of only a few or small clusters of human cells in the injured mouse brains of our study is in agreement with this hypothesis as well.

Recently, evidence of sexual-dimorphism in responses to other sources of stem cells, including embryonic stem cells, mesenchymal stem cells, and endothelial progenitor stem cells, have been reviewed in adult models of cardiovascular disease [24,25]. In these stem cell populations, sex-related differences were noted in the levels of growth factors released and receptors expressed. To our knowledge, there are no reports regarding sex-related differences in CB stem cells and responses to them. In the data reported here, the noted sex-related differences in SGZ cell proliferation, glial, and microglial responses to the CB treatment were not associated with in the severity of stroke injury between male and female injured pups. Therefore, the sex-related differences in these treatment responses are likely due to a difference in how the CB stem cells respond to stroke injury in the male versus female pup, or alternatively how the male versus female stroke-injured pup responds to the cells.

Ischemic injury in the immature brain is known to be sexually dimorphic in rodents; in male pups ischemic brain injury predominately proceeds through an AIF-mediated pathway and in females via predominately caspase-dependent pathways [26]. Therefore, treatments that preferentially block one of these pathways produce a sex-dependent response [27]. How these pathways may relate to the mechanism of CB stem cell-treatment effects is not known at this time, but this issue should be further studied. Neurogenesis in the developing rat hippocampus is also sexually dimorphic; as early as 1 week of life the male hippocampus is larger than the female. This larger size is associated with more neurons and with more glia (in CA3) in males, and with differences in hippocampal levels of estradiol, testosterone, and dihydrotesterone compared with females [28,29]. Therefore, the sexually dimorphic hippocampus in the immature rodent may be primed to differently respond to ischemia or to growth factors released by the human CBSC. Neurogenesis in the SVZ is also sexually dimorphic. However, this has only been described in postpubertal rodents [30], and is associated with differences in hormonal levels.

A recent study suggests that sexually dimorphic cytokine responses to a LPS insult in vitro may be seen in astrocytes taken from P1 CD1 mice. It may be that there are sexually dimorphic astrocytic responses after an ischemic injury as well, and a sexually dimorphic astrocyte response could in turn prompt sexually dimorphic responses from CB stem cells. The increase in GFAP expression after cell treatment in the region of the SVZ of females and in the granule cell layer and hilus of the DG of males may represent an increased astrocytic response and an increase in progenitor labeling; the increased GFAP in SVZ proper likely primarily represents an increase in progenitor labeling. Further studies with co-labeling of GFAP expressing cells with markers to delineate progenitors (such as DCX and NG2) and astrocytes (such as GLAST and ALDHD1L1) are needed to further elucidate the identity of cells producing the sexually dimorphic response in GFAP. Our prior studies suggest that increased poststroke SVZ cell proliferation in this model results in increased generation of new astrocytes [9]. However, the role of astrocytes in the recovery after stroke in the immature brain is complex with some functions that protect and others that endanger neurons [31]. Therefore, additional studies are needed to determine whether the sexually dimorphic SVZ and SGZ GFAP expression in response to the CB treatment results in better (or worse) chronic recovery. The data, at this time point at least, indicate an impact of the CB cells upon astroglial responses after stroke injury in the immature brain, thereby directing attention for future studies to the sex differences in the astroglial response within the neurogenic niches.

The altered correlations between spleen weights and both injury and cell proliferation may support a role for the CD34$^+$-enriched cell fraction in modulating poststroke immune responses as previously reported [16]. It has been shown that peripheral inflammatory cells are recruited from the spleen in response to the stroke, invade the brain and contribute to evolution of the injury [32,33]. Human CB cells studied in rat stroke models have reported amelioration of the stroke-induced reduction in spleen size [16]. Additionally, anti-inflammatory properties of CB cells have been reported by altered expression of cytokines in the spleen of ischemic rats [34].

The primary focus of this study was the impact on proliferation in the neurogenic niches and the behavioral outcomes were added in an attempt to expand the outcomes of this study. It is unclear at this point whether or not the sexually dimorphic increases in SGZ and SVZ proliferation are beneficial. A follow-up study is planned that will follow the effect of treatment out to P60 with behavioral testing at about P50, which will determine the impact of CBSC upon cognitive impairments already published in this model. Very few studies have explored the therapeutic potential of human CB therapy in stroke in an immature brain [35]. In the neonatal models, human CB cells have been infused either intravenously or intraperitoneally at time points ranging from 3 h to 7 days after the stroke with no significant reductions in the size of infarct [36–39]. Improved motor outcomes, however, were reported in most but not all the rat studies. Our study did not find evidence that CBSC treatment resulted in early functional improvement, as measured by improved weight gain or open-field testing. However, most of our functional outcome measures were insensitive to the brain injury and therefore unable to assess response to treatment. We previously demonstrated in this model that newborn cells in the SGZ after stroke injury become mature dentate granule neurons, and a cell subset integrate into visual-spatial memory circuits after stroke [40]. However, additional work is needed to determine whether the increased SGZ cell proliferation in males, 9 days after stroke and 7 days after CBSC treatment, results in an increase in SGZ neurons, which mature and appropriately integrate. Because it takes about 3–4 weeks for newborn SGZ neurons that survive to migrate to the granule cell layer and manifest a high rate of glutamatergic synaptogenesis, Arc expression, and connectivity [40,41], future studies will determine whether the sex-dependent effects of cord blood-derived stem cells result in long-term cognitive improvements,

impairments, or increases the chances of developing epilepsy, which has been shown to occur in this model [40]. Future studies should consider keeping animals for 8 weeks or more post ischemia to assess effects of treatment. Other tasks that might be useful to assess the impact of the CB stem cell treatment include cognitive testing such as the T-maze and novel object testing.

It is possible that a higher dose of cells would produce a greater effect. Other possible approaches, to increase the beneficial effect with regards to reducing the stroke injury and improving outcomes, include considering intraparenchymal or intraventricular injection, compared with the mesenchymal stem cell fraction or whole mononuclear fraction in this model, and administering along with a drug to break down the BBB. These different approaches are just starting to be studied and more work is needed to optimize the parameters for CB stem cell therapy after stroke in the immature brain, particularly in humans.

There are limitations to this study that suggest venues in need of further study. This study did not evaluate the host immune responses to the human xenografts. It is possible that the endogenous immune response to the systemic xenograft had a role in producing the results noted, and that the data may have been different had the animals been immunosuppressed. Most other studies of human CB cells in immature rodent models do not immunosuppress since this will significantly modify the ischemic process. Also, previously published studies of human CB cells in neonatal models have not reported the sex of the donor human infant and we were not provided with this information from the anonymous human source. Sex-related differences have been reported in human CB cells [42]. It is possible that the majority of the CB units were either male or female and therefore the sex-dependent differences could relate to this variable; this information was unavailable to us for these de-identified samples and therefore we were unable to analyze this variable. There could be a different host immune response to the CBSC depending on whether male or female CBSC are injected into a male or female animal. Alternatively, CBSC could release different cytokines in response to the stroke injury depending on whether the cell is derived from a male or female baby. Future studies will need to investigate and control this variable.

We attempted to label cord blood-derived cells with primary antibodies against human antigens (generated in mice) including HuNu, $CD34^+$, and HuMit. We conclude from these experiments that all of these markers showed non-specific labeling in these experiments where there is high level of infiltration of monophagocytic cells in the mouse brains; a few such cells were even seen in vehicle-treated uninjured brains. It is possible that the exogenous human cells infiltrated the injured side and that these antibodies stained both mouse and human CB-derived cells. However, it is also possible that the human cells have been eliminated by this time point by the mouse immune response, and that this immune response generated by the mouse to the human cells was important in modifying the brain injury. Future studies are needed to address these possibilities.

Recent clinical trials utilizing either autologous or allogeneic CB cells for the treatment of cerebral palsy in humans have both demonstrated functional benefit [43,44].The use of allogeneic CBSC, while more generally available as a treatment, is also more risky in that an immune response to the graft may be generated. However, the authors, of the study reporting the results of a double-blinded placebo controlled study of CB plus erythropoietin and rehabilitation versus placebo plus erythropoietin and rehabilitation versus two placebos and rehabilitation, hypothesized that the positive effect of the autologous CB cells upon functional outcome was likely related to the disease-modifying effects of the immune response generated by the host to the transplanted cells [44].

SGZ cells proliferation was increased in ligation injured at 9 days poststroke in contrast to our previous study 7 days poststroke [9]. In our previous studies, the pups remained in their home cages with the dam and were not handled until the day of sacrifice. However, in this study the pups underwent daily handling for the experimental protocols. This enrichment may account for the poststroke upregulation of SGZ neurogenesis seen in all the injured groups in this study and is consistent with previous studies demonstrating that enriched environments and exercise modulates endogenous neurogenesis in a sex-dependent manner. Since all groups received the same handling and testing, this would not account for sex-related differences in results noted in the CBSC-treated injured animals compared to the vehicle-treated injured animals.

In summary, CBSC resulted in an increase in SGZ neurogenesis in the males, an increase in contralateral SVZ region proliferation and evidence of sex-dependent modulation of the poststroke neuro-glial immune response. These data encourage further study to determine the mechanisms underlying these results and the relevance of these effects to chronic functional and pathologic outcomes. In addition, it is essential that future studies of CBSC, where possible, note the sex of the human infant CB source to determine whether this contributes to sex-dependent effects.

Acknowledgments

This study was supported by the MSCRF: RFA-MD-09-2 (AMC), R01 NS061969 (AMC), R01 NS 28208 (MVJ), and 5K08NS063956-02 (ASF). We thank Kathy Mintz for her valuable technical assistance in $CD34^+$ cell enrichment and Tayana Verina for her technical assistance with $CD34^+$ and HuNu antibody labeling. We also thank the INOVA Fairfax Hospital Cord Blood collection for providing the research human CB units.

Author Disclosure Statement

No competing financial interests exist.

References

1. Koelfen W, M Freund and V Varnholt. (1995). Neonatal stroke involving the middle cerebral artery in term infants: clinical presentation, EEG and imaging studies, and outcome. Dev Med Child Neurol 37:204–212.
2. Calza L, M Fernandez, A Giuliani, S Pirondi, G D'Intino, M Manservigi, N De Sordi and L Giardino. (2004). Stem cells and nervous tissue repair: from in vitro to in vivo. Prog Brain Res 146:75–91.
3. Majka M, A Janowska-Wieczorek, J Ratajczak, K Ehrenman, Z Pietrzkowski, MA Kowalska, AM Gewirtz, SG Emerson and MZ Ratajczak. (2001). Numerous growth

factors, cytokines, and chemokines are secreted by human CD34$^+$ cells, myeloblasts, erythroblasts, and megakaryoblasts and regulate normal hematopoiesis in an autocrine/paracrine manner. Blood 97:3075–3085.
4. Mohle R, F Bautz, S Rafii, MA Moore, W Brugger and L Kanz. (1998).The chemokine receptor CXCR-4 is expressed on CD34$^+$ hematopoietic progenitors and leukemic cells and mediates transendothelial migration induced by stromal cell-derived factor-1. Blood 91:4523–4530.
5. Naiyer AJ, DY Jo, J Ahn, R Mohle, M Peichev, G Lam, RL Silverstein, MA Moore and S Rafii. (1999). Stromal derived factor-1-induced chemokinesis of cord blood CD34$^+$ cells (long-term culture-initiating cells) through endothelial cells is mediated by E-selectin. Blood 94:4011–4019.
6. Comi AM, CJ Weisz, BH Highet, MV Johnston and MA Wilson. (2004). A new model of stroke and ischemic seizures in the immature mouse. Pediatr Neurol 31:254–257.
7. Comi AM, BH Highet, P Mehta, HT Chong, MV Johnston and MA Wilson. (2006) Dextromethorphan protects male but not female mice with brain ischemia. Neuroreport 17:1319–1322.
8. Gilland E, E Bona and H Hagberg. (1998) Temporal changes of regional glucose use, blood flow, and microtubule-associated protein 2 immunostaining after hypoxia-ischemia in the immature rat brain. J Cereb Blood Flow Metab 18:222–228.
9. Kadam, SD, JD Mulholland, JW McDonald and AM Comi. (2008). Neurogenesis and neuronal commitment following ischemia in a new mouse model for neonatal stroke. Brain Res 1208:35–45.
10. Hill JM, MA Lim and Stone MM. Developmental milestones in the newborn mouse. Neuropeptide Tech 2007:131–149.
11. Choi YS, MY Lee, KW Sung, SW Jeong, JS Choi, HJ Park, ON Kim, SB Lee and SY Kim. (2003). Regional differences in enhanced neurogenesis in the dentate gyrus of adult rats after transient forebrain ischemia. Mol Cells 16:232–238.
12. Paxinos G and KM Franklin. (2009). *The Mouse Brain in Stereotaxic Coordinates*, 2nd edn. Academic Press, San Diego, CA.
13. Kadam SD, JD Mulholland, JW McDonald and AM Comi. (2009). Poststroke subgranular and rostral subventricular zone proliferation in a mouse model of neonatal stroke. J Neurosci Res 87:2653–2666.
14. Verina T, CA Rohde and TR Guilarte. (2007). Environmental lead exposure during early life alters granule cell neurogenesis and morphology in the hippocampus of young adult rats. Neuroscience 145:1037–1047.
15. Chen SH, FM Chang, HK Chang, WC Chen, KF Huang and MT Lin. (2007). Human umbilical cord blood-derived CD34$^+$ cells cause attenuation of multiorgan dysfunction during experimental heatstroke. Shock 27:663–671.
16. Chen J, PR Sanberg, Y Li, L Wang, M Lu, AE Willing, J Sanchez-Ramos and M Chopp. (2001). Intravenous administration of human umbilical cord blood reduces behavioral deficits after stroke in rats. Stroke 32:2682–2688.
17. Vendrame M, C Gemma, KR Pennypacker, PC Bickford, Davis C Sanberg, PR Sanberg and AE Willing. (2006). Cord blood rescues stroke-induced changes in splenocyte phenotype and function. Exp Neurol 199:191–200.
18. Van Epps DE, J Bender, W Lee, M Schilling, A Smith, S Smith, K Unverzaqt, P Law and J Burgess. (1994). Harvesting, characterization, and culture of CD34$^+$ cells from human bone marrow, peripheral blood, and cord blood. Blood Cells 20:411–423.
19. Chen N, JE Hudson, P Walczak, I Misiuta, S Garbuzova-Davis, L Jiang, Sanchez-J Ramos, PR Sanberg, T Zigova and AE Willing. (2005). Human umbilical cord blood progenitors: the potential of these hematopoietic cells to become neural. Stem Cells 23:1560–1570.
20. Newcomb JD, CT Ajmo, Jr., CD Sanberg, PR Sanberg, KR Pennypacker and AE Willing. (2006). Timing of cord blood treatment after experimental stroke determines therapeutic efficacy. Cell Transplant 15:213–223.
21. Boltze J, UR Schmidt, DM Reich, A Kranz, KG Reymann, M Strassburger, D Lobsien, DC Wagner, A Förschler and WR Schäbitz. (2011). Determination of the therapeutic time window for human umbilical cord blood mononuclear cell transplantation following experimental stroke in rats. Cell Transplant 21:1199–1211.
22. Borlongan CV, M Hadman, C vis Sanberg and PR Sanberg. (2004). Central nervous system entry of peripherally injected umbilical cord blood cells is not required for neuroprotection in stroke. Stroke 35:2385–2389.
23. Arien-Zakay H, S Lecht, MM Bercu, R Tabakman, R Kohen, H Galski, A Nagler and P Lazarovici. (2009). Neuroprotection by cord blood neural progenitors involves antioxidants, neurotrophic and angiogenic factors. Exp Neurol 216:83–94.
24. Herrmann JL, AM Abarbanell, BR Weil, MC Manukyan, JA Poynter, Y Wang, AC Coffey and DR Meldrum. (2010). Gender dimorphisms in progenitor and stem cell function in cardiovascular disease. J CardiovascTransl Res 3:103–113.
25. Lecanu L. (2011) Sex, the underestimated potential determining factor in brain tissue repair strategy. Stem Cells Dev 20:2031–2035.
26. Sharma J, G Nelluru, MA Wilson, MV Johnston and MA Hossain. (2011). Sex-specific activation of cell death signalling pathways in cerebellar granule neurons exposed to oxygen glucose deprivation followed by reoxygenation. ASN Neuro 3:2.
27. Nijboer CH, F Groenendaal, A Kavelaars, HH Hagberg, F van Bel and CJ Heijnen. (2006). Gender-specific neuroprotection by 2-iminobiotin after hypoxia-ischemia in the neonatal rat via a nitric oxide independent pathway. J Cereb Blood Flow Metab 27:282–292.
28. Zhang JM, AT Konkle, SL Zup and MM McCarthy. (2008). Impact of sex and hormones on new cells in the developing rat hippocampus: a novel source of sex dimorphism? Eur J Neurosci 27:791–800.
29. Bowers JM, J Waddell and MM McCarthy. (2010). A developmental sex difference in hippocampal neurogenesis is mediated by endogenous oestradiol. Biol Sex Differ 1:8.
30. Kim JY P Casaccia-Bonnefil. (2009). Interplay of hormones and p53 in modulating gender dimorphism of subventricular zone cell number. J Neurosci Res 87:3297–3305.
31. Barreto G, RE White, Y Ouyang, L Xu and RG Giffard. (2011). Astrocytes: targets for neuroprotection in stroke. Cent Nerv Syst Agents Med Chem 11:164–173.
32. Ajmo CT, Jr., DOL Vernon, L Collier, AA Hall, S Garbuzova-Davis, A Willing and KR Pennypacker. (2008). The spleen contributes to stroke-induced neurodegeneration. J Neurosci Res 86:2227–2234.
33. Bao Y, E Kim, S Bhosle, H Mehta and S Cho. (2010). A role for spleen monocytes in post-ischemic brain inflammation and injury. J Neuroinflammation 7:92.
34. Vendrame M, C Gemma, D de Mesquita, L Collier, PC Bickford, CD Sanberg, PR Sanberg, KR Pennypacker and AE Willing. (2005). Anti-inflammatory effects of human cord blood cells in a rat model of stroke. Stem Cells Dev 14:595–604.

35. Pimentel-Coelho PM and R Mendez-Otero. (2010). Cell therapy for neonatal hypoxic-ischemic encephalopathy. Stem Cells Dev 19:299–310.
36. de Paula S, AS Vitola, S Greggio, D de Paula, PB Mello, JM Lubianca, LL Xavier, HH Fiori and JC Dacosta. (2009). Hemispheric brain injury and behavioral deficits induced by severe neonatal hypoxia-ischemia in rats are not attenuated by intravenous administration of human umbilical cord blood cells. Pediatr Res 65:631–635.
37. Meier C, J Middelanis, B Wasielewski, S Neuhoff, A Roth-Haerer, M Gantert, HR Dinse, R Dermietzel and A Jensen. (2006). Spastic paresis after perinatal brain damage in rats is reduced by human cord blood mononuclear cells. Pediatr Res 59:244–249.
38. Pimentel-Coelho PM, ES Magalhaes, LM Lopes, LC deAzevedo, MF Santiago and R Mendez-Otero. (2009). Human cord blood transplantation in a neonatal rat model of hypoxic-ischemic brain damage: functional outcome related to neuroprotection in the striatum. Stem Cells Dev 19:351–358.
39. Yasuhara T, K Hara, M Maki, L Xu, G Yu, MM Ali, T Masuda, SJ Yu, EK Bae, et al. (2009). Mannitol facilitates neurotrophic factor upregulation and behavioral recovery in neonatal hypoxic-ischemic rats with human umbilical cord blood grafts. J Cell Mol Med 14:914–921.
40. Kadam SD, CL Smith-Hicks, DR Smith, PF Worley and AM Comi. (2010). Functional integration of new neurons into hippocampal networks and poststroke comorbidities following neonatal stroke in mice. Epilepsy Behav 18: 344–357.
41. Piatti VC, MG Davies-Sala, MS Esposito, LA Mongiat, MF Trinchero and AF Schinder. (2011). The timing for neuronal maturation in the adult hippocampus is modulated by local network activity. J Neurosci 31:7715–7728.
42. Wasiluk A, K Ratomski, K Wnuczko, J Zak, M Szczepański, J Wysocka and EA Jasińska. (2009). Expression of FasR, Fas-L and Bcl-2 in $CD4^+$ and $CD8^+$ subpopulations of T lymphocytes in the cord blood of healthy full-term newborns, is gender of influence? Adv Med Sci 54: 99–103.
43. Lee YH, KV Choi, JH Moon, HJ Jun, HR Kang, SI Oh, HS Kim, JS Um, MJ Kim, et al. (2012). Safety and feasibility of countering neurological impairment by intravenous administration of autologous cord blood in cerebral palsy. J Transl Med 10:58.
44. Min K, J Song, JY Kang, J Ko, JS Ryu, MS Kang, SJ Jang, SH Kim, D Oh, MK Kim, SS Kim and M Kim. (2013). Umbilical cord blood therapy potentiated with erythropoietin for children with cerebral palsy: a double-blind, randomized, placebo-controlled trial. Stem Cells 31:581–591.

Address correspondence to:
Dr. Anne M. Comi
Department of Neurology and Developmental Medicine
Kennedy Krieger Research Institute
KKI-553, 801N, Broadway
Baltimore, MD 21205

E-mail: comi@kennedykrieger.org

Received for publication March 18, 2014
Accepted after revision August 7, 2014
Prepublished on Liebert Instant Online August 14, 2014